water

MDPI

Article

Investigating the Change Pattern in Adsorption Properties of Soil Media for Non-Polar Organic Contaminants under the Impact of Freezing and Thawing

Jingjing Huang [1,2,3], Rong Zhong [1,2,3] and Hang Lyu [1,2,3,*]

[1] Key Laboratory of Groundwater Resources and Environment, Ministry of Education, Jilin University, Changchun 130026, China; huangjj9920@mails.jlu.edu.cn (J.H.); zhongrong21@mails.jlu.edu.cn (R.Z.)
[2] Jilin Provincial Key Laboratory of Water Resources and Environment, Jilin University, Changchun 130026, China
[3] Institute of Water Resources and Environment, Jilin University, Changchun 130021, China
* Correspondence: lvhangmail@163.com; Tel.: +137-5602-9934

Abstract: The adsorption of petroleum hydrocarbons by soils in the unsaturated zone determines the amount that goes into the groundwater. However, the intricate behavior of petroleum hydrocarbon adsorption in soil media under the influence of freeze–thaw conditions in globally prevalent seasonally frozen regions remains unclear. Alkanes as a non-polar compound are an important part of petroleum hydrocarbons. We conducted field-scale seasonal freeze-thaw experiments using n-dodecane to quantify the dynamic patterns and influencing factors of the physicochemical properties of soil media and their adsorption capacity for petroleum hydrocarbons during different freeze–thaw cycles. Our findings demonstrated that, as the number of natural freeze–thaw cycles increased, the proportion of soil micro-agglomerates rose rapidly, thereby expanding the available adsorption sites and enhancing the adsorption capacity for non-polar organic pollutants. The rise in sorption capacity for the outdoor freeze–thaw experimental group surpassed that of the indoor room-temperature control group by an impressive 75.57%, showing the enhancement of the adsorption capacity for non-polar organic pollutants. Conversely, the decline in soil organic matter content during the later stages of the freeze–thaw process hampered its adsorption performance for non-polar organic pollutants. The decrease in sorption capacity for the outdoor freeze–thaw experimental group surpassed that of the indoor room temperature control group by 77.97%. By shedding light on the adsorption mechanisms of non-polar organic pollutants in soils subjected to freeze–thaw conditions, our research facilitated a comprehensive understanding and predictive modeling of this process. Furthermore, our study provided a scientific foundation for exploring the convergence and migration transformation patterns of other organic compounds in petroleum-contaminated areas within seasonally frozen regions.

Keywords: freezing and thawing; non-polar organic contaminants; adsorption; soil physicochemical properties

Citation: Huang, J.; Zhong, R.; Lyu, H. Investigating the Change Pattern in Adsorption Properties of Soil Media for Non-Polar Organic Contaminants under the Impact of Freezing and Thawing. *Water* **2023**, *15*, 2515. https://doi.org/10.3390/w15142515

Academic Editors: Maurizio Barbieri, Yuanzheng Zhai and Jin Wu

Received: 2 June 2023
Revised: 28 June 2023
Accepted: 5 July 2023
Published: 9 July 2023

1. Introduction

Petroleum, as a versatile raw material for numerous industries, currently stands as one of the foremost energy sources [1]. However, the irrational extraction and utilization of petroleum can lead to inadvertent leaks and releases, permeating the underground soil and water environment via urban pipelines, underground storage tanks, and other pathways [2]. Extensive research has demonstrated that adsorption plays a pivotal role in the entrapment of petroleum hydrocarbons within the soil, significantly influencing their transport dynamics [3,4]. This phenomenon greatly determines the sequestration process of contaminants in the unsaturated zone, as well as the threat posed to groundwater resources. For instance, the Golmud region in China exhibits elevated concentrations of petroleum

hydrocarbons in its groundwater. Through the exclusion of human activities as a factor, it has been observed that the aquifer lithology in this region is characterized by loose, coarse-grained, and highly permeable characteristics, which can impede the adsorption of petroleum hydrocarbons and render them more prone to enter the groundwater system [5]. Petroleum hydrocarbons are categorized as alkanes, cycloalkanes, and aromatics. Alkanes, as non-polar compounds, are an important part of petroleum hydrocarbons [6]. The results of our testing and analysis of the composition and content of petroleum hydrocarbon contamination at the site found that alkanes accounted for the highest percentage of total petroleum hydrocarbons in groundwater, with an average of 65.6% of the total oil percentage, specifically including dodecane and pentadecane. Therefore, studying the adsorption processes of non-polar organic contaminants within the subsurface unsaturated zone can be of paramount importance in safeguarding groundwater environments and effectively managing petroleum pollution.

The adsorption mechanisms of organic pollutants in the soil encompass a range of phenomena, such as electrostatic interactions, hydrogen bonding, hydrophobic bonding, van der Waals forces, donor-acceptor mechanisms, and ligand exchange, etc. These mechanisms synergistically operate and compete, ultimately determining the fate of organic pollutant adsorption in soil [7]. Non-polar organic contaminants, classified as hydrophobic organic chemicals, are subject to the influence of both organic matter content and environmental factors present within the soil [8–14]. Soil organic matter, characterized by a heterogeneous mixture of diverse organic compounds consisting of hydrophilic and hydrophobic constituents, exerts a significant impact on the adsorption behavior of non-polar organic contaminants. The hydrophobic effect induces the formation of complexes between organic matter and hydrogen bonding, thus increasing the availability of adsorption sites within the soil. Consequently, as the hydrophobicity of organic matter intensifies, the soil exhibits a heightened capacity for adsorbing non-polar organic contaminants [15]. The pH levels also exert an influence on the charge of soil colloids and the distribution patterns of petroleum contaminants. Studies have revealed that, in acidic solutions, contaminants can establish hydrogen bonds with carboxyl and phenolic hydroxyl groups present in organic matter, thereby facilitating the adsorption process [7,16]. Furthermore, the stability of soil aggregates plays a crucial role in retaining soil organic matter. The enhanced stability of soil aggregates correlates with higher levels of organic matter content within the soil [17]. Overall, variations in soil pH and aggregate stability can impact the organic matter content of the soil, which can subsequently influence its affinity for organic pollutants, thereby modulating the adsorption properties of the soil medium.

Seasonal permafrost is extensively distributed worldwide, exhibiting an average of 50.5% of the total land area in the Northern Hemisphere, as well as reaching 81% during extremely cold years [18,19]. Freeze–thaw cycles, as abiotic stressors impacting the soil, possess the capacity to basically alter soil states to influence soil structure and water distribution characteristics, which can subsequently affect the sorption processes of contaminants. Although current research primarily focuses on the adsorption processes under freeze–thaw conditions for heavy metals, studies involving organic pollutants are relatively limited. Dang et al. [20] discovered that freeze–thaw cycles can significantly impact dissolved organic matter, agglomerates, and pore ratios in soils, leading to reduced sorption capacity for Cd, thereby promoting vertical migration and morphological transformations. Wang, X et al. [21] observed through laboratory batch experiments that pH, organic matter content, and free iron oxide content exhibited negative correlations with freeze-thaw frequency, resulting in diminished sorption capacity for soil Pb and Cd compared to unfrozen soil. This can consequently raise the risk of heavy metal contamination in groundwater. Yang et al. [22] revealed that the number and duration of freeze–thaw cycles influenced the strength properties and chemical stability of solidified/stabilized lead-contaminated soil. The freezing and thawing processes can induce alterations in the physicochemical properties of soil media. Existing research on the transport of organic pollutants under freezing and thawing conditions primarily concentrates on indoor experiments [23–25]. However,

there remains a relative dearth of research examining the effects of freeze–thaw action on soil adsorption of organic pollutants under natural conditions. Neglecting the influence of freezing and thawing on the organic pollutant adsorption process may significantly cause the predicted result range of soil groundwater organic pollution to deviate from the actual scenario, substantially impacting the risk assessment and remediation strategies for organic pollutants contamination in groundwater.

Building upon this foundation, this study delved into the changes in the adsorption properties of soil media regarding non-polar organic pollutants under the influence of the natural freeze–thaw processes. Through the execution of field-based freeze–thaw experiments within a seasonally frozen region, we conducted adsorption tests on soil samples across various freeze–thaw stages while also assessing the physical and chemical property indices of the soil. The research objectives were to comprehensively characterize the alterations in non-polar organic pollutant adsorption properties within soils at different freeze–thaw stages under natural conditions and to discern the key factors influencing the adsorption capacity of soils for non-polar organic pollutants in the context of freeze–thaw action.

2. Experimental Materials and Methods

2.1. Materials

To better simulate the change pattern of non-polar organic pollutants adsorption under real soil conditions, the unpolluted areas at the designated field test site, characterized by a relatively flat and stable terrain with flourishing vegetation, were selected for conducting the random sampling process. Considering that the adsorption of non-polar organic contaminants by soil occurs mostly on the soil surface, three sampling points were randomly identified with the selection of surface soil samples from a depth of 0 to 20 cm. Subsequently, the soil samples obtained from different sampling points were thoroughly mixed. These samples were then transported to a shaded indoor laboratory for the air-drying process. During this process, visible debris, such as fallen leaves and roots, were meticulously removed from the soil. The dried soil was sieved through a 2-mm mesh and stored in sealed plastic bags for subsequent analysis. Because the highest percentage of alkanes in the total petroleum hydrocarbons in the groundwater of the sampling site, accounting for 65.6% of the total oil percentage on average, specifically including dodecane and pentadecane, the study selected dodecane as the typical alkane pollutant of petroleum hydrocarbon at the site. For the experiments, methanol (Tianjin Fuyu Fine Chemical Co., Ltd., Tinjin, China), n-dodecane (Tianjin Kemiou Chemical Reagent Co., Ltd., Tianjin, China), and dichloromethane (Tianjin Fuyu Fine Chemical Co., Ltd., Tinjin, Chian) of analytical purity were employed as reagents, whereby n-dodecane was dissolved in methanol to prepare the stock solution, and di-chloromethane was used to extract n-dodecane from the aqueous solution, while the water used was all ultrapure water.

2.2. Experimental Design

The experimental setup consisted of two distinct components, including an outdoor experimental group and an indoor control group, each comprising five soil samples. The outdoor group aimed to observe the dynamic changes in soil properties and its adsorption capacity for pollutants over the course of the winter season under natural conditions. In contrast, the indoor control group was established to isolate the effects of non-freezing and thawing conditions. Uniform filling methods were employed for both the outdoor and indoor soil columns, with each column containing 500 g of dry soil (including the amount used for parallel indicator samples). The soil columns were filled in accordance with the volume corresponding to the desired moisture content of 15%. Layered additions of soil and water were created during the filling process, followed by a 24-h equilibration period at room temperature to ensure uniform moisture distribution. In total, 11 soil columns were filled, with one column designated for the determination of initial values; as well, the remaining columns were divided into two groups. For the latter two-group

soil columns, five of them for the outdoor group were deployed at the field test site on 19 November 2022 (at the beginning of November, the temperature at the test site gradually dropped to below zero, and the samples were made and placed on the site on 19 November), while the remaining five columns were placed in the indoor laboratory as control samples. Probes were utilized to monitor both site temperature and soil temperature changes, and the sampling interval was adjusted accordingly. Probes were utilized to monitor both site temperature and soil temperature changes, and the sampling interval was adjusted accordingly. The first sample was collected on 29 November 2022, followed by subsequent samples on 9 December 2022, 9 January 2023, 9 February 2023, and 12 March 2023. To facilitate the comparison of the results of different groups, the outdoor samples were labeled as K1–K5, whereas the indoor samples were labeled as D1–D5. Following retrieval, the samples were dried in shaded conditions in preparation for the subsequent processing. The samples after retrieval at different time points needed to be dried indoors for subsequent analytical processing.

2.3. Measurement of Sample Indicators

2.3.1. Adsorption Kinetics Parameters

The equilibrium adsorption quantities and corresponding adsorption rates of non-polar organic contaminants adsorbed by soil were determined through adsorption kinetic experiments. These experiments aimed to analyze the process of non-polar organic contaminant adsorption by soil under both freeze–thaw conditions and indoor ambient conditions. To ensure the stability of n-dodecane in the solvent, methanol was selected as the solvent to prepare a stock solution of n-dodecane with a concentration of 20 g/L. Additionally, a 0.01 mol/L $CaCl_2$ solution was prepared to establish ionic equilibrium in the soil prior to commencing the adsorption experiments. Based on preliminary experiments, a soil-to-water ratio of 1:25 was determined as the appropriate ratio. For each experimental run, 2 g of treated soil were weighed into a series of 50 mL centrifuge tubes, followed by the addition of 50 mL of the prepared $CaCl_2$ solution to minimize headspace. The tubes were then placed on an oscillator and shaken overnight to allow the soil to achieve ionic equilibrium prior to the initiation of adsorption. Subsequently, the n-dodecane stock solution was added to achieve an initial concentration of 0.2 g/L in each centrifuge tube; after that, they were put in the oscillator again. In sampling after a specific interval (5, 15, 35, 65, 125, 275, 515, 1440, and 2880 min), the supernatant of the centrifuged sample was extracted and dichloromethane was added to extract the n-dodecane from the supernatant, during which the sample was fully extracted using ultrasound. The resulting samples were transferred to 1.5 mL agilent vials, and the concentration of n-dodecane was determined using gas chromatography (Agilent 7890B/5977B). Parallel experiments were conducted under identical conditions for comparison and validation.

2.3.2. Physical and Chemical Properties of Media

To further analyze the pattern of variations in the adsorption performance, several parameters, including pH, agglomerate composition, and the soil organic carbon (SOC) index, were measured in the soil samples from both the outdoor and control groups. A 10 g soil sample was weighed in a beaker, and 25 mL of ultrapure water were added. The mixture was vigorously stirred for 2 min and left undisturbed for 30 min. Within 1 h, the pH of the solution was measured using a pH meter (Thunder PHSJ 6L). To assess the changes in soil agglomerates during the winter season, the soil was divided into three particle-size ranges: 2–0.3 mm, 0.3–0.25 mm, and <0.25 mm. The agglomerates of each particle-size range were individually weighed (Sieve Shaker, POWTEQ SS2000). The SOC content was determined using the Elementar vario MACRO cube (German), which provided an accurate measurement of soil organic carbon.

2.4. Data Analysis

To examine the variations in the sorption process of non-polar organic contaminants by soil across various sampling nodes and under varying conditions, the sorption quantity was employed to represent the sorption at a specific time node. In addition, the sorption kinetic equation was utilized to analyze the sorption characteristics of organic pollutants. The intraparticle diffusion adsorption kinetics model is one of the most widely used adsorption kinetics models (also cited as the "Weber–Morris model" and the "IPD model" in some published papers) [17,26,27]. Furthermore, the mean weight diameter (MWD) of soil agglomerates pertaining to various particle sizes served as an indicator of soil agglomerate stability. The WDM was calculated by referring to the method of Yonker et al. [28]. The calculation of the adsorption kinetics parameters and MWD were conducted using the following formula:

Adsorption amount:

$$q_c = \frac{(C_0 - C_t)V}{M} \tag{1}$$

pseudo-first-order kinetics:

$$lg(q_e - q_c) = lgq_e - \frac{k_1}{2.303}t \tag{2}$$

pseudo-second-order kinetics:

$$\frac{t}{q_c} = \frac{1}{k_2 q_e^2} + \frac{1}{q_e}t \tag{3}$$

intraparticle diffusion model:

$$q_c = k_{id}t^{1/2} + C \tag{4}$$

where C_0 represents the initial concentration of n-dodecane (g/L); C_t represents the concentration of the n-dodecane at moment t (g/L); V denotes the volume of the solution (L); M represents the mass of the soil (kg); t represents the time (min); q_c represents the amount of n-dodecane adsorbed at moment t (g/kg); q_e represents the amount of n-dodecane adsorbed on the soil surface at equilibrium, i.e., the equilibrium adsorption capacity (g/kg); k_1 represents the rate constant of pseudo-first-order sorption (min^{-1}); k_2 represents the rate constant of pseudo-second-order sorption ($kg{\cdot}g^{-1}{\cdot}min^{-1}$); k_{id} represents the intraparticle diffusion rate constant $g/(kg{\cdot}min^{-1/2})$; and C represents the intercept.

MWD:

$$\text{MWD} = \sum_1^n (x_i \times W_i) \tag{5}$$

where x_i, W_i, and n denote the average diameter of soil agglomerates (mm), the proportion of each particle-size agglomerate to the total sample, and the number of agglomerate components, respectively.

3. Results and Discussion

3.1. Patterns of Air and Soil Temperature Changes during the Freeze–Thaw Period

The air temperature and surface soil temperature exhibited typical seasonal dynamics at the field experiment site spanning from 1 November 2022 to 15 March 2023 (Figure 1). Notably, temperatures started to decrease significantly on November 11, reaching sub-zero levels on 25 November, as well as with the lowest temperature recorded on 24 January 2023. Temperature fluctuations persisted until March 2023, when temperatures began to rise above zero again. The temperature fluctuations observed in different soil depths were generally consistent, with the surface layer (0.2 cm) displaying significantly smaller temperature variations than the overall temperature changes. The soil temperature decreased to 0 °C for the first time on 5 December, with a 10-day delay compared to the air temperature. The soil temperature at the depth of 10 cm was 3–4 °C higher than that at the depth of 0.2 cm, indicating a gradual decline in heat transfer between the atmosphere and the soil. Although the soil temperature was influenced by the air temperature, there existed

a certain lag and diminishing response of soil temperature to changes in air temperature. Freezing was considered to occur from the surface downwards, and the adsorption of surface non-polar organic contaminants in the soil primarily occurred in the soil surface layer. Based on the 0.2 cm soil temperature, the winter–spring phases of freeze–thaw cycles in 2022–2023 were categorized as follows: the first freeze-thaw cycle period from 5 December to 14 December 2022; the freezing period from 15 December 2022 to 27 February 2023; and the second freeze–thaw cycle period from 28 February to 5 March.

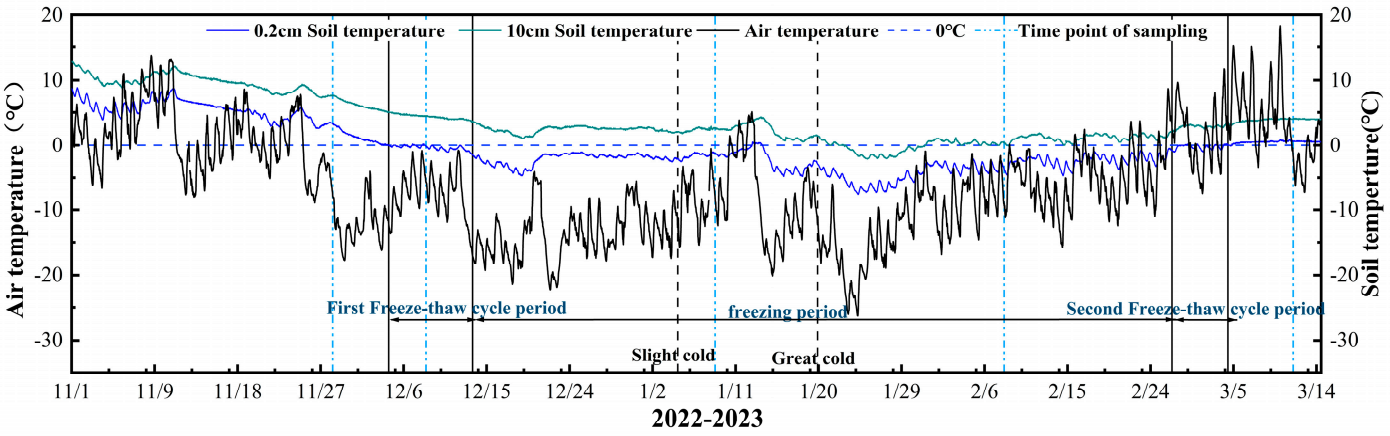

Figure 1. Schematic diagram of air temperature and soil temperature (2022–2023).

During the first freeze–thaw cycle, the soil surface temperature exhibited constant fluctuations around 0 °C. This freeze–thaw period spanned 9 days, with a temperature range between −0.6 °C and 0.2 °C. Overall, four freeze–thaw cycle processes occurred. Upon entering the subsequent freezing period, the soil temperature remained below 0 °C. However, there was an exceptional weather event during the period between Lesser Cold (5 January) and Greater Cold (20 January), when the temperature suddenly rose above 0 °C. Consequently, the 0.2 cm soil temperature also increased above zero. However, this occurrence lasted only 2 days, without subsequent fluctuations above or below 0 °C. Therefore, the impact of temperature changes on the soil during this period was disregarded. Following a soil freezing period of 54 days, the temperature gradually rose from sub-zero levels to above zero, signifying the entering of the second freeze–thaw cycle period. At this stage, a total of five freeze–thaw cycles were observed, spanning six days, with a freeze–thaw temperature range of −0.9 °C–0.5 °C.

3.2. Changes in Sorption Capacity of Non-Polar Organic Contaminants in Soils during Freeze–Thaw Conditions

Both the outdoor experimental samples and the indoor control samples reached adsorption equilibrium within 1500 min at different times during the freeze–thaw period. The measured equilibrium sorption amounts for each month, from 29 November 2022 to 12 March 2023, were 973.1, 996.1, 992.5, 996.0, and 920.0 g/kg for the outdoor experimental group, as well as 976.9, 990.0, 995.3, 990.0, and 931.0 g/kg for the indoor ambient control group during the same period, respectively. In general, the equilibrium sorption capacities of both the outdoor experimental group and the indoor control group exhibited a decreasing trend over time, with the final equilibrium sorption capacity of the outdoor experimental group being lower than that of the indoor control group (Figure 2). This indicates that freeze–thaw action can affect the non-polar organic contaminants' sorption performance of the soil media. To explore the adsorption mechanism of non-polar organic contaminants adsorbed by soils under freeze–thaw conditions, we employed the pseudo-first order kinetics model and pseudo-second order kinetics model. The correlation between $lg(q_e q_t)$ and t for both the outdoor freeze–thaw test group and the indoor room temperature control group did not conform to a linear relationship. Therefore, it was concluded that the process of soil adsorption of non-polar organic contaminants did not follow a pseudo-

first-order kinetics model, but rather a pseudo-second-order kinetics model (Table 1). The pseudo-first-order kinetics model involved a physical process as the rate-limiting step, while the pseudo-second-order kinetics model relied on chemical processes [29]. Organic pollutants underwent transfer, exchange, or electron sharing with molecules or atoms on the soil surface, leading to the formation of adsorption chemical bonds. To further understand the key processes controlling the adsorption of non-polar organic contaminants from soils, we investigated the relationship between q_c and $t^{1/2}$ based on the theoretical intraparticle diffusion model proposed by Weber and Morris [17]. If the graph of $t^{1/2}$-q_c followed a curve passing through the origin, it indicated that soil adsorption of non-polar organic contaminants was primarily accomplished by intra-particle diffusion, where the rate of inter-particle diffusion affected the rate of soil adsorption of non-polar organic contaminants [30,31]. The change patterns of the inter-particle diffusion model plots for both the outdoor experimental group and the indoor control group were consistent (Figure 3). These plots were not linear over time while they exhibited two linear straight lines, which suggested that the adsorption process of non-polar organic contaminants in soil during the freeze–thaw period can be divided into two steps: surface adsorption and intra-particle diffusion. Initially, non-polar organic contaminants were adsorbed on the outer surface of the soil, and when the outer surface became saturated, the hydrocarbons penetrated the inner soil particles and were adsorbed by the inner surface [32]. Hence, the adsorption rate of soil non-polar organic contaminants was influenced by both the adsorption rate on the soil surface and the intra-particle adsorption rate. Soil adsorption of non-polar organic contaminants was a chemisorption process involving adsorption on the soil surface and diffusion adsorption within the particles, where molecules or atoms on the soil surface and within the particles formed chemisorption bonds with non-polar organic contaminants.

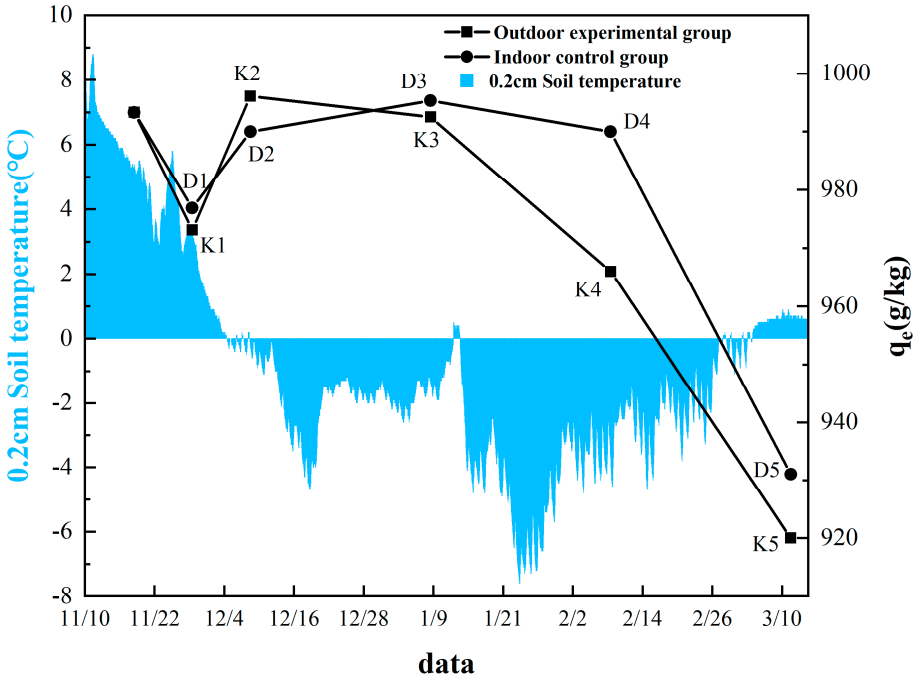

Figure 2. Time-dependent equilibrium adsorption amount.

Table 1. Kinetic constants and correlation coefficients for kinetic models.

Pseudo-First Order										**Pseudo-Second Order**								
Outdoor Experimental Group					**Indoor Control Group**					**Outdoor Experimental Group**					**Indoor Control Group**			
Time	$q_{e,\mathbf{exp}}$	$q_{e,\mathbf{cal}}$	$\mathbf{k_2}$	$\mathbf{R^2}$	**Time**	$q_{e,\mathbf{exp}}$	$q_{e,\mathbf{cal}}$	k_2	$\mathbf{R^2}$	**Time**	$q_{e,\mathbf{exp}}$	$q_{e,\mathbf{cal}}$	k_2	$\mathbf{R^2}$	**Time**	$q_{e,\mathbf{exp}}$	$q_{e,\mathbf{cal}}$	k_2	$\mathbf{R^2}$
initial	993.30	63.35	2.50×10^{-3}	0.39982	initial	993.30	63.35	2.50×10^{-3}	0.39982	initial	993.30	1000.00	1.85×10^{-4}	0.99997	initial	993.30	1000.00	1.85×10^{-4}	0.99990
K1	973.10	144.66	1.02×10^{-5}	0.23509	D1	976.90	146.08	9.42×10^{-6}	0.13102	K1	973.10	961.54	5.85×10^{-5}	0.99883	D1	976.90	990.10	1.63×10^{-4}	0.99990
K2	996.10	178.62	3.20×10^{-3}	0.82961	D2	990.00	139.88	2.70×10^{-3}	0.76586	K2	996.10	1000.00	1.25×10^{-4}	0.99998	D2	990.00	961.54	7.69×10^{-5}	0.99980
K3	992.50	221.89	3.70×10^{-3}	0.85827	D3	995.30	143.41	3.30×10^{-3}	0.78954	K3	992.50	1000.00	7.58×10^{-5}	0.99989	D3	995.30	1000.00	1.40×10^{-4}	0.99990
K4	966.00	269.26	4.40×10^{-3}	0.85287	D4	990.00	140.20	2.50×10^{-3}	0.54376	K4	966.00	970.87	9.71×10^{-5}	0.99997	D4	990.00	990.10	1.07×10^{-4}	0.99990
K5	920.00	267.33	2.90×10^{-3}	0.81663	D5	931.00	459.07	2.50×10^{-3}	0.84052	K5	920.00	925.93	9.36×10^{-5}	0.99965	D5	931.00	943.40	2.29×10^{-4}	0.99640

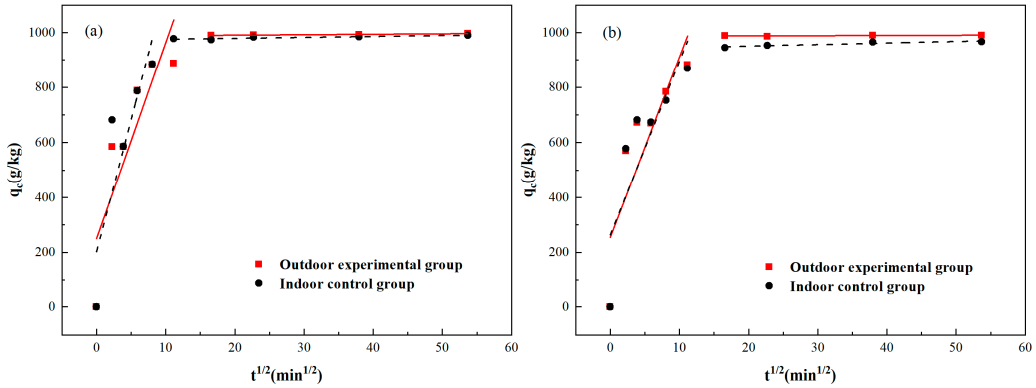

Figure 3. Intraparticle diffusion model (**a**) 9 December 2022; (**b**) 9 February 2023.

Prior to entering the freeze–thaw period, the equilibrium sorption capacity of both the outdoor experimental group and the indoor ambient group exhibited a decline with the continuous decrease in soil temperature. However, it is noteworthy that the equilibrium adsorption capacity of D1 (29th November) under indoor room temperature conditions only decreased by 16.4 g/kg compared to the initial value. In contrast, K1 under outdoor freeze–thaw conditions experienced a decrease of 20.2 g/kg compared to the initial value during the same period, representing a 23.17% larger decrease than that observed for D1. As the outdoor temperature gradually decreased prior to the freeze–thaw period, the soil underwent a chemisorption process to adsorb non-polar organic contaminants. The lowered temperature resulted in a decrease in energy and a slowdown in the movement of non-polar organic contaminant molecules. Consequently, the adsorption between non-polar organic contaminants and soil was weakened, as evidenced by the 23.17% reduction in the equilibrium adsorption capacity of the outdoor experimental group compared to the indoor room temperature group.

During the initial freeze–thaw cycle, K2 (9th December) exposed to outdoor freeze–thaw conditions experienced three consecutive freeze–thaw cycles, exhibiting an equilibrium sorption capacity of 996.1 g/kg. Conversely, D2, subjected to indoor ambient conditions during the same period, demonstrated a sorption capacity of 990.0 g/kg. Remarkably, the rise in sorption capacity for K2 surpassed that of the D2 group by an impressive 75.57%. Throughout the first freeze–thaw cycle, soil temperature fluctuated intermittently above and below the freezing point (0 °C). This dynamic temperature variation induced continuous transitions between solid and liquid states of soil moisture, consequently disrupting the structure of soil agglomerates. The resulting fragmentation led to the formation of smaller agglomerates, which in turn increased the availability of adsorption sites on the soil surface. Consequently, this facilitated the enhanced adsorption of non-polar organic contaminants by the soil.

Following the freezing period and two subsequent freeze–thaw cycle phases, K5 (12th March) exposed to outdoor freeze–thaw conditions underwent a total of 9 freeze–thaw cycles, ultimately attaining a final equilibrium adsorption capacity of 920.0 g/kg. In contrast, D5, placed under indoor room temperature conditions during the same period, achieved a final equilibrium adsorption capacity of 931.0 g/kg. Notably, the prolonged freezing and freeze–thawing of K5 resulted in a significantly lower equilibrium sorption capacity than D5. The extended exposure to a low-temperature environment with multiple freeze–thaw cycles induced alterations in various physicochemical properties of the soil, resulting in a diminished adsorption capability for non-polar organic contaminants. When the soil was frozen, its hydraulic conductivity experienced a substantial reduction, leading to the formation of an impermeable ice layer. This impeded the diffusion of organic pollutants within the soil and restricted their interaction with the soil matrix, thereby diminishing the sorption of non-polar organic contaminants in the outdoor experimental group during the freezing period. Furthermore, the occurrence of multiple freeze–thaw cycles can disrupt the soil structure, resulting in reduced soil stability and a decline in

organic matter content. These factors collectively contributed to a decrease in adsorption capacity. The formation of an ice barrier during the freezing period, coupled with the decrease in soil organic matter content due to multiple freeze–thaw cycles, synergistically reduced the sorption properties of the soil matrix towards non-polar organic contaminants under final outdoor freeze–thaw conditions.

3.3. Analysis of Factors Influencing Sorption Capacity of Soils for Non-Polar Organic Contaminants during the Freeze–Thaw Period

In the conducted experiment, the pH fluctuation range observed under outdoor freeze–thaw conditions was narrower compared to indoor room temperature conditions. Notably, the final pH of K5 (12th March) exposed to outdoor freeze–thaw conditions was lower than that of D5 subjected to indoor room temperature conditions (Figure 4b). The agglomerates present in the soil were classified into three categories based on particle size: large agglomerates (2–0.3 mm), small agglomerates (0.3–0.25 mm), and micro-agglomerates (less than 0.25 mm). Throughout the experiment, there was a consistent overall increase in the percentage of micro-agglomerates under outdoor freeze–thaw conditions, while the percentage of large agglomerates exhibited a slight decrease (Figure 4a). Specifically, after the first freeze–thaw cycle period, the percentage of micro-agglomerates reached its peak value (65.66%) at K2 (9th December) under outdoor freeze–thaw conditions, whereas the percentage of large agglomerates dropped to its minimum value (14.41%). Moreover, the WMD of the agglomerates also reached its lowest value (30.26 mm) and subsequently fluctuated upwards. The overall SOC content under outdoor freeze–thaw conditions was lower compared to that of indoor room temperature conditions, primarily due to the destabilization of soil agglomerates. Specifically, the final SOC content of K5 (12th March) exposed to outdoor freeze–thaw conditions was 48.47 mg/kg, which was lower than the SOC content of D5 (51.80 mg/kg) subjected to indoor room temperature conditions during the same period.

During the initial freeze–thaw cycle, K2 subjected to outdoor freeze–thaw conditions underwent three consecutive freeze–thaw cycles, resulting in an increase in the proportion of small and micro-agglomerates within the soil. This led to a peak adsorption capacity of non-polar organic contaminants at 996.1 g/kg. Concurrently, the pH of the soil rose from 7.83 to 7.92, while the SOC content decreased from 47.73 mg/kg to 43.23 mg/kg. The process of freeze–thawing promoted the preferential adsorption of H^+ ions by organic matter, thereby contributing to an elevation in soil pH. Moreover, the freeze–thaw cycle induced the continuous transition of soil water between liquid and solid states, ultimately resulting in the disruption of soil aggregate structure. This led to the fragmentation of large aggregates into micro-aggregates and the subsequent loss of cementation between agglomerate particles, thereby reducing their stability [33]. Since SOC can be predominantly stored within agglomerates, the decrease in agglomerate stability led to a decline in SOC content [34]. On December 9th, the percentage of micro-agglomerates in K2 reached 65.66%, while large agglomerates accounted for only 14.41% under outdoor freeze–thaw conditions. Similarly, under indoor room temperature conditions, the percentage of micro-agglomerates in D3 was 57.44%, with large agglomerates comprising 20.13%. It can be evident that, following the first freeze–thaw cycle period, the increase in pH and decrease in SOC content under outdoor freeze–thaw conditions mitigated the organic matter's ability to adsorb non-polar organic contaminants. However, the rise in the proportion of micro-agglomerates within the soil provided additional adsorption sites for non-polar organic contaminants, collectively enhancing the soil's capacity to adsorb these hydrocarbons.

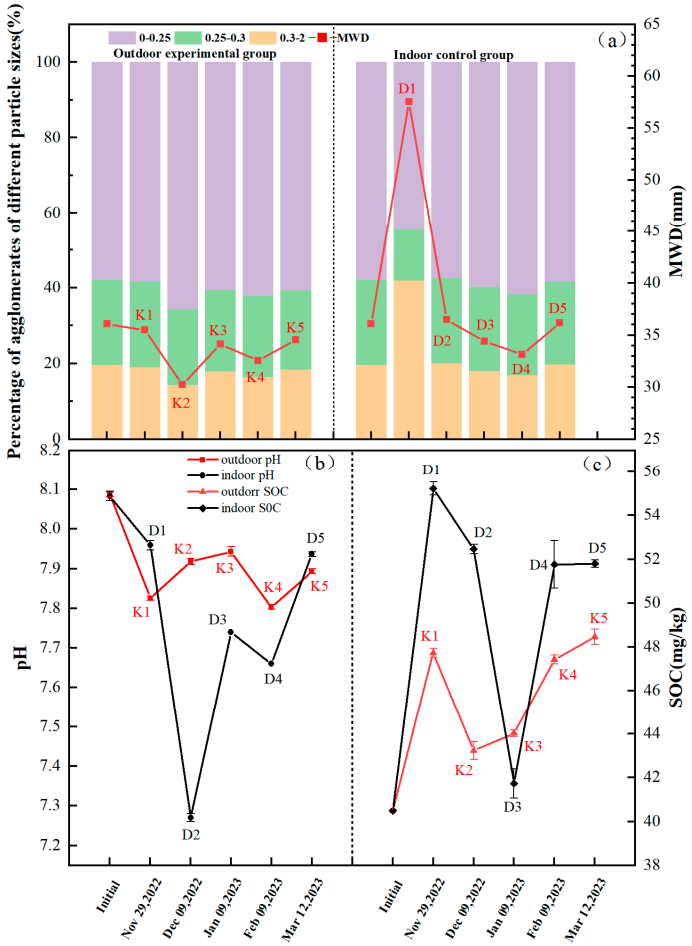

Figure 4. Changes in physical and chemical properties of soil indoors and outdoors. (**a**) Indoor and outdoor changes in the ratio of different particle-size agglomerates to MWD. (**b**) Indoor and outdoor soil pH changes. (**c**) Indoor and outdoor SOM content changes.

Following the completion of the second freeze–thaw cycle period, K5 (12 March) exposed to outdoor freeze–thaw conditions experienced a total of 9 freeze–thaw cycles. It was observed that the soil agglomerate stability remained lower compared to D5 subjected to indoor ambient conditions during the same period, indicating that multiple freeze–thaw cycles reduced agglomerate stability. Concurrently, the pH and SOC contents of the final K5 were lower than those of D5 under room temperature conditions in the corresponding period. However, the percentage of agglomerates did not exhibit a significant difference between the two groups. The freeze–thaw cycle disrupted soil aggregates, releasing dissolved organic matter and soil colloids. Additionally, it stimulated low-temperature stress responses in soil microorganisms, promoting nitrification reactions and the release of dissolved organic acids. This, in turn, increased H+ concentration in the soil solution [35]. The decrease in soil pH enhanced the adsorption of soil organic carbon to hydrophobic organic matter. This occurred due to the dissociation of carboxyl and hydroxyl groups of organic matter under alkaline conditions, resulting in an increase in net negative charge and enhancing the hydrophilicity of soil organic matter. Consequently, the affinity of soil organic matter towards hydrophobic organic matter was reduced [13,36,37]. The SOC, a crucial component of soil organic matter (SOM), declined because of freeze–thaw cycles. The SOM was recognized as a vital adsorption medium for organic compounds in soil [38,39]. The lower the organic matter content in the soil, the weaker the adsorption properties of the soil towards non-polar organic contaminants. Although the proportion of agglomerates of different particle sizes did not differ significantly, the decrease in pH caused by freeze–thaw action can enhance the adsorption affinity of soil organic matter towards non-polar organic

contaminants. At the same time, the reduction in soil stability and organic carbon content led to a decrease in SOM, consequently resulting in a decline in the soil's adsorption capacity for non-polar organic contaminants. Hence, after the completion of two freeze–thaw cycle periods, the equilibrium adsorption capacity of the outdoor experimental group was significantly lower than that of the indoor room temperature group.

In summary, the freeze–thaw cycle exerted an impact on the distribution of agglomerates of various particle sizes within the soil. It induced the fragmentation of large agglomerates and consequently increased the proportion of micro-agglomerates. This, in turn, enhanced the number of adsorption sites for non-polar organic contaminants in the soil, thereby improving the overall adsorption performance of the soil media for these hydrocarbons. Additionally, the freeze–thaw process influenced the pH levels in the soil. The breakup of agglomerates during freeze–thaw released organic acids, leading to an elevation in H^+ concentration in the soil. As a result, the adsorption affinity of organic matter towards non-polar organic contaminants was enhanced. However, the freeze–thaw cycle destabilizes soil agglomerates, leading to a reduction in organic matter content and subsequently decreasing the amount of non-polar organic contaminants adsorbed by the organic matter. Following three freeze–thaw cycles, there was a notable increase in the proportion of soil micro-agglomerates, thereby augmenting the adsorption sites for non-polar organic contaminants in the soil and resulting in improved adsorption properties. However, after nine freeze–thaw cycles, the ratios of soil agglomerates stabilized, and the decline in SOC content led to a decrease in sorption performance. In the pre-freeze–thaw period, the increased proportion of micro-agglomerates increased the sorption of non-polar organic pollutants by the soil, but at the same time the increase in pH and the decrease in SOC content weakened the sorption capacity of the soil. The combined effect of these two factors resulted in a small difference between the indoor and outdoor soil sorption capacity during the pre-freeze–thaw period. While the ratio of micro-agglomerates in indoor and outdoor soils remained stable during the late freeze–thaw cycle, the reduction of SOC content in the outdoor group greatly weakened the sorption capacity of its soils. This makes the difference between the sorption capacity of indoor and outdoor soils for non-polar organic pollutants in the late stage. Overall, as the number of freeze–thaw cycles increased, alterations in soil physicochemical properties initially enhanced the non-polar organic contaminant adsorption properties of the soil, while eventually they contributed to a decline in these properties.

4. Conclusions

In this study, we conducted monitoring of physical and chemical properties of soils and their variations in a non-polar organic contaminant adsorption capacity during the freezing and thawing cycles in a seasonal frozen region (from November 2022 to March 2023). In the pre-freeze–thaw period, the proportion of ruptured microaggregates in the soil increased, leading to the release of organic acids and lowering the pH. The acidic environment enhanced the ability of soil organic matter to adsorb non-polar organic pollutants. Meanwhile, the increased proportion of micro-agglomerates provided additional adsorption sites for non-polar organic contaminants, thereby improving the overall adsorption performance of the soil medium. However, with continued freeze–thaw cycles, the stability of the agglomerates decreased, resulting in a reduction in organic matter content within the soil. This, in turn, mitigated the adsorption capacity of organic matter for non-polar organic contaminants, leading to a decrease in the soil's overall adsorption performance for these hydrocarbons. In summary, the freeze–thaw process demonstrated a significant impact on the distribution of aggregates of varying particle sizes and the organic matter content within the soil, consequently influencing the sorption of non-polar organic contaminants by the soil. In the pre-freeze–thaw period, the effect of the soil on non-polar organic pollutants is mainly influenced by the proportion of soil aggregates, while in the later period, it is mainly influenced by the organic matter content of the soil. This research shed light on the adsorption patterns of non-polar organic contaminants under freeze–thaw conditions,

which can be vital for the prediction of groundwater petroleum hydrocarbon pollution in seasonal permafrost areas as well as in designing effective remediation strategies. Moreover, it can help reduce prediction errors resulting from the effects of freeze–thaw cycles. However, the coupling between the changes of the physicochemical properties of the packaged gas zone media and the adsorption of petroleum hydrocarbons under the freeze–thaw effect needs to be further investigated through indoor experiments.

Author Contributions: Conceptualization, H.L.; Data curation, R.Z.; Formal analysis, J.H.; Investigation, J.H. and R.Z.; Methodology, H.L., J.H. and R.Z.; Resources: J.H. and R.Z.; Writing—original draft: J.H.; Writing—review & editing: H.L. and R.Z.; Supervision: H.L. All authors have read and agreed to the published version of the manuscript.

Funding: This research is supported by the National Natural Science Foundation of China (U19A20107, 42172267, 42230204).

Data Availability Statement: Not applicable.

Conflicts of Interest: The authors declare no conflict of interest.

References

1. Varjani, S.J.; Upasani, V.N. Carbon spectrum utilization by an indigenous strain of *Pseudomonas aeruginosa* NCIM 5514: Production, characterization and surface active properties of biosurfactant. *Bioresour. Technol.* **2016**, *221*, 510–516. [CrossRef] [PubMed]
2. Aislabie, J.; Saul, D.J.; Foght, J.M. Bioremediation of hydrocarbon-contaminated polar soils. *Extremophiles* **2006**, *10*, 171–179. [CrossRef] [PubMed]
3. Pu, X.C.; Cutright, T.J. Sorption–desorption behavior of PCP on soil organic matter and clay minerals. *Chemosphere* **2006**, *64*, 972–983. [CrossRef] [PubMed]
4. An, S.; Woo, H.; Kim, S.H.; Yun, S.T.; Chung, J.; Lee, S. Complex behavior of petroleum hydrocarbons in vadose zone: A holistic analysis using unsaturated soil columns. *Chemosphere* **2023**, *326*, 138417. [CrossRef] [PubMed]
5. Qiao, X.C.; Zheng, B.H.; Li, X.; Zhao, X.R.; Dionysiou, D.D.; Liu, Y. Influencing factors and health risk assessment of polycyclic aromatic hydrocarbons in groundwater in China. *J. Hazard. Mater.* **2021**, *402*, 123419. [CrossRef]
6. Wang, M.; Ding, M.; Yuan, Y. Bioengineering for the Microbial Degradation of Petroleum Hydrocarbon Contaminants. *Bioengineering* **2023**, *10*, 347. [CrossRef]
7. Ertli, T.; Marton, A.; Földényi, R. Effect of pH and the role of organic matter in the adsorption of isoproturon on soils. *Chemosphere* **2004**, *57*, 771–779. [CrossRef]
8. Cornelissen, G.; Rigterink, H.; Ferdinandy, M.M.A.; Van Noort, P.C.M. Rapidly desorbing fractions of PAHs in contaminated sediments as a predictor of the extent of bioremediation. *Environ. Sci. Technol.* **1998**, *32*, 966–970. [CrossRef]
9. Li, Q.; Zhao, D.; Yin, J.; Zhou, X.; Li, Y.; Chi, P.; Han, Y.; Ansari, U.; Cheng, Y. Sediment instability caused by gas production from hydrate-bearing sediment in Northern South China Sea by horizontal wellbore: Evolution and mechanism. *Nat. Resour. Res.* **2023**, *32*, 1595–1620. [CrossRef]
10. Li, Q.; Zhang, C.; Yang, Y.; Ansari, U.; Han, Y.; Li, X.; Cheng, Y. Preliminary experimental investigation on long-term fracture conductivity for evaluating the feasibility and efficiency of fracturing operation in offshore hydrate-bearing sediments. *Ocean Eng.* **2023**, *281*, 114949. [CrossRef]
11. Wang, F.; Liu, X.; Jiang, B.; Zhuo, H.; Chen, W.; Chen, Y.; Li, X. Low-loading Pt nanoparticles combined with the atomically dispersed FeN4 sites supported by FeSA-NC for improved activity and stability towards oxygen reduction reaction/hydrogen evolution reaction in acid and alkaline media. *J. Colloid Interface Sci.* **2023**, *635*, 514–523. [CrossRef]
12. Luthy, R.G.; Aiken, G.R.; Brusseau, M.L.; Cunningham, S.D.; Gschwend, P.M.; Pignatello, J.J.; Reinhard, M.; Traina, S.J.; Weber, W.J. Sequestration of hydrophobic organic contaminants by geosorbents. *Environ. Sci. Technol.* **1997**, *31*, 3341–3347. [CrossRef]
13. Pil-Gon, K.I.M.; Tarafdar, A.; Jung-Hwan, K. Effect of soil pH on the sorption capacity of soil organic matter for polycyclic aromatic hydrocarbons in unsaturated soils. *Pedosphere* **2023**, *33*, 365–371.
14. Lamoureux, E.M.; Brownawell, B.J. Chemical and biological availability of sediment-sorbed hydrophobic organic contaminants. *Environ. Toxicol. Chem.* **1999**, *18*, 1733–1741. [CrossRef]
15. Ehlers, G.A.C.; Forrester, S.T.; Scherr, K.E.; Loibner, A.P.; Janik, L.J. Influence of the nature of soil organic matter on the sorption behaviour of pentadecane as determined by PLS analysis of mid-infrared DRIFT and solid-state 13C NMR spectra. *Environ. Pollut.* **2010**, *158*, 285–291. [CrossRef]
16. Chiou, C.T.; Porter, P.E.; Schmedding, D.W. Partition equilibriums of nonionic organic compounds between soil organic matter and water. *Environ. Sci. Technol.* **1983**, *17*, 227–231. [CrossRef]
17. Weber Jr, W.J.; Morris, J.C. Kinetics of adsorption on carbon from solution. *J. Sanit. Eng. Div.* **1963**, *89*, 31–59. [CrossRef]
18. Park, J.; Kwon, O.S.; Di Sarno, L. Influence of seasonal soil temperature variation and global warming on the seismic response of frozen soils in permafrost regions. *Earthq. Eng. Struct. Dyn.* **2021**, *50*, 3855–3871. [CrossRef]

19. Tokuda, D.; Kim, H.; Yamazaki, D.; Oki, T. Development of a global river water temperature model considering fluvial dynamics and seasonal freeze-thaw cycle. *Water Resour. Res.* **2019**, *55*, 1366–1383. [CrossRef]
20. Dang, X.L.; Zhang, Y.L.; Yu, N.; Zhang, Y.L. Cadmium adsorption-desorption of brown soil with freeze–thaw cycles in northeast China. *Int. J. Environ. Pollut.* **2012**, *49*, 89–99. [CrossRef]
21. Wang, X.; Li, Y.M.; Mao, N.; Zhou, Y.Q.; Guo, P. The adsorption behavior of Pb^{2+} and Cd^{2+} in the treated black soils with different freeze-thaw frequencies. *Water Air Soil Pollut.* **2017**, *228*, 193. [CrossRef]
22. Yang, Z.P.; Zhang, K.S.; Li, X.Y.; Ren, S.P.; Li, P. The effects of long-term freezing–thawing on the strength properties and the chemical stability of compound solidified/stabilized lead-contaminated soil. *Environ. Sci. Pollut. Res.* **2023**, *30*, 38185–38201. [CrossRef]
23. Zhao, Q.; Xing, B.S.; Tai, P.D.; Yang, K.; Li, H.; Zhang, L.Z.; Lin, G.; Li, P.J. Effect of freeze–thawing cycles on aging behavior of phenanthrene, pyrene and their mixture in soil. *Sci. Total Environ.* **2013**, *452*, 246–252. [CrossRef] [PubMed]
24. Zhao, Q.; Li, P.J.; Stagnitti, F.; Ye, J.; Dong, D.B.; Zhang, Y.Q.; Li, P. Effects of aging and freeze-thawing on extractability of pyrene in soil. *Chemosphere* **2009**, *76*, 447–452. [CrossRef]
25. Zhao, Q.; Weise, L.; Li, P.J.; Yang, K.; Zhang, Y.Q.; Dong, D.B.; Li, P.; Li, X.J. Ageing behavior of phenanthrene and pyrene in soils: A study using sodium dodecylbenzenesulfonate extraction. *J. Hazard. Mater.* **2010**, *183*, 881–887. [CrossRef] [PubMed]
26. Erdoğan, B.C.; Ülkü, S. Cr (VI) sorption by using clinoptilolite and bacteria loaded clinoptilolite rich mineral. *Microporous Mesoporous Mater.* **2012**, *152*, 253–261. [CrossRef]
27. Zhuang, S.; Zhu, K.; Xu, L.; Hu, J.; Wang, J. Adsorption of Co^{2+} and Sr^{2+} in aqueous solution by a novel fibrous chitosan biosorbent. *Sci. Total Environ.* **2022**, *825*, 153998. [CrossRef]
28. Yonker, R.E.; McGuinness, J.L. A Short Method of Obtaining Mean Weight Diameter Values of Aggregate Analysis of Soil. *Soil Sci.* **1957**, *83*, 291–294.
29. Mohan, D.; Singh, K.P.; Singh, V.K. Trivalent chromium removal from wastewater using low cost activated carbon derived from agricultural waste material and activated carbon fabric cloth. *J. Hazard. Mater.* **2006**, *135*, 280–295. [CrossRef]
30. Wang, J.L.; Guo, X. Rethinking of the intraparticle diffusion adsorption kinetics model: Interpretation, solving methods and applications. *Chemosphere* **2022**, *309*, 136732. [CrossRef]
31. Saleh, T.A.; Siddiqui, M.N.; Al-Arfaj, A.A. Kinetic and intraparticle diffusion studies of carbon nanotubes-titania for desulfurization of fuels. *Pet. Sci. Technol.* **2016**, *34*, 1468–1474. [CrossRef]
32. Söenmezay, A.; Öncel, M.S.; Bektas, N. Adsorption of lead and cadmium ions from aqueous solutions using manganoxide minerals. *Trans. Nonferr. Metal. Soc. China* **2012**, *22*, 3131–3139. [CrossRef]
33. Edwards, L.M. The effect of alternate freezing and thawing on aggregate stability and aggregate size distribution of some Prince Edward Island soils. *J. Soil Sci.* **1991**, *42*, 193–204. [CrossRef]
34. Guan, S.; Dou, S.; Chen, G.; Wang, G.; Zhuang, J. Isotopic characterization of sequestration and transformation of plant residue carbon in relation to soil aggregation dynamics. *Appl. Soil Ecol.* **2015**, *96*, 18–24. [CrossRef]
35. van Bochove, E.; Prévost, D.; Pelletier, F. Effects of freeze–thaw and soil structure on nitrous oxide produced in a clay soil. *Soil Sci. Soc. Am. J.* **2000**, *64*, 1638–1643. [CrossRef]
36. Yang, F.; Wang, M.; Wang, Z.Y. Sorption behavior of 17 phthalic acid esters on three soils: Effects of pH and dissolved organic matter, sorption coefficient measurement and QSPR study. *Chemosphere* **2013**, *93*, 82–89. [CrossRef]
37. Li, B.H.; Qian, Y.; Bi, E.P.; Chen, H.H.; Schmidt, T.C. Sorption behavior of phthalic acid esters on reference soils evaluated by soil column chromatography. *Clean* **2010**, *38*, 425–429. [CrossRef]
38. Wang, X.L.; Guo, X.Y.; Yang, Y.; Tao, S.; Xing, B.S. Sorption mechanisms of phenanthrene, lindane, and atrazine with various humic acid fractions from a single soil sample. *Environ. Sci. Technol.* **2011**, *45*, 2124–2130. [CrossRef]
39. Kołtowski, M.; Hilber, I.; Bucheli, T.D.; Oleszczuk, P. Effect of activated carbon and biochars on the bioavailability of polycyclic aromatic hydrocarbons in different industrially contaminated soils. *Environ. Sci. Pollut. Res.* **2016**, *23*, 11058–11068. [CrossRef]